Exp Brain Res (1993) 95:223–239

Experimental Brain Research

Principal cells of the rat medial nucleus of the trapezoid body: an intracellular in vivo study of their physiology and morphology

Inken Sommer, Kurt Lingenhöhl*, Eckhard Friauf

Department of Animal Physiology, University of Tübingen, Auf der Morgenstelle 28, D-72076 Tübingen, Germany

Received: 10 November 1992 / Accepted: 16 March 1993

Abstract. The medial nucleus of the trapezoid body (MNTB) is one of several principal nuclei in the superior olivary complex (SOC) of mammals. It is classically thought to function as a relay station between the contralateral ventral cochlear nucleus and the lateral superior olive (LSO), playing a role among those brainstem nuclei that are involved in binaural hearing. In order to characterise the physiology and morphology at the cellular level of the major neuronal component of the MNTB, the principal cells, we have analysed these neurons in rats in vivo using intracellular recordings and horseradish peroxidase-labelling. Our data demonstrate that MNTB principal cells, when being stimulated acoustically via the contralateral ear, show a phasic-tonic response with an onset latency of 3.5 ms and a suppression of their spontaneous activity following stimulus offset. These neurons have an axonal morphology whose complexity has not yet been described. All cells ($n=10$) projected exclusively ipsilaterally and had terminal axonal arbors in a variety of auditory brainstem nuclei. At least two and maximally seven auditory targets were innervated by an individual cell. Each cell projected into the LSO and the superior paraolivary nucleus (SPN). Additional projections that were intrinsic to the SOC were often observed in the lateral nucleus of the trapezoid body and in periolivary regions, with only one cell projecting into the medial superior olive. Most, if not all, MNTB principal cells also had projections that were extrinsic to the SOC, as their axons ascended into the lateral lemniscus. In two neurons the ascending axon formed terminal arbors in the ventral nucleus of the lateral lemniscus, and the dorsal nucleus of the lateral lemniscus could be identified as a target of one neuron. The location of the cell bodies of the MNTB principal cells correlated with the neurons' best frequencies, thereby demonstrating a tonotopic organisation of the MNTB, with high frequencies being represented medially and low frequencies laterally. The axonal projections into the LSO and the SPN were also tonotopically organised and the alignment of the tonotopic axes was similar to that in the MNTB. Our results confirm previous data from other species and suggest that MNTB principal cells have a great amount of physiological and morphological similarities across mammalian species. Furthermore, the complexity of the axonal projections indicates that these neurons play a role in auditory information processing which goes far beyond their previously described classical role.

Key words: Superior olivary complex – Lateral superior olive – Nucleus of the lateral lemniscus – Periolivary regions – Rat

Introduction

The medial nucleus of the trapezoid body (MNTB) is a prominent nucleus in the auditory brainstem and comprises the largest cell group in the superior olivary complex of several mammalian species (Casey and Feldman 1985; Spangler et al. 1985). Based on Golgi and EM studies in the cat, Morest (1968) described three neuronal types in the MNTB, the stellate, elongate and principal cells. Most of the literature has focused on the principal cells, which form, by far, the major proportion of the MNTB cells (82% in the rat, Casey and Feldman 1982). Principal cells are oval or globular neurons with fine, dispersed Nissl substance, an eccentric nucleus and few slender dendrites (Taber 1961; Morest 1968). They receive their main excitatory input through a characteristic, large and calyx-like axosomatic synapse, the "calyx of Held", which was originally described 100 years ago (Held 1893). The calyces of Held originate from large diameter, myelinated trapezoid body axons which arise from globular bushy cells in the contralateral ventral cochlear nucleus (VCN: Harrison and Warr 1962; Warr 1972; Friauf and Ostwald, 1988; Spirou et al. 1990; Kuwabara et al. 1991; Smith et al. 1991).

Present address: * Ciba-Geigy AG, PO Box, CH-4002 Basel, Switzerland

Correspondence to: E. Friauf

Efferent projections of MNTB principal cells to the ipsilateral lateral superior olive (LSO) are well described and appear to be present in all mammalian species (cat, Morest 1968; Elverland 1978; Glendenning et al. 1985; Spangler et al. 1985; Smith et al. 1989; rabbit, Borg 1973; kangaroo rat, Browner and Webster 1975; guinea pig, Bledsoe et al. 1988; gerbil, Kuwabara and Zook 1991; Sanes and Siverls 1991; mouse, big brown bat, moustache bat, Zook and DiCaprio 1988; Kuwabara and Zook 1991; rat, Banks and Smith 1992). There is compelling evidence that MNTB principal neurons are glycinergic (reviews: Caspary and Finlayson 1991; Wenthold 1991) and thus can inhibit LSO neurons (Saint Marie et al. 1989; Wu and Kelly 1992). Electrophysiological data which show that the contralateral acoustic input to LSO neurons is inhibitory (Tsuchitani and Boudreau 1966; Guinan et al. 1972b; Caird and Klinke 1983) and can be blocked by the glycine antagonist strychnine (Moore and Caspary 1983) corroborate this contention. Due to the excitatory input from the contralateral VCN and the inhibitory output to the LSO, MNTB principal cells are classically thought to function as a relay station in the ascending auditory system, converting excitatory information from the contralateral VCN into inhibitory input to neurons in the LSO (Irvine 1986; Helfert et al. 1991).

Aside from the primary projection to the LSO, projections from MNTB neurons to other auditory brainstem nuclei, all located ipsilaterally, have also been described using various tracing techniques. Auditory target nuclei of MNTB neurons include the ventral and dorsal nucleus of the lateral lemniscus (VNLL and DNLL, Glendenning et al. 1981; Spangler et al. 1985; Bledsoe et al. 1988), the medial superior olive (MSO), the superior paraolivary nucleus (SPN), the lateral nucleus of the trapezoid body (LNTB, Bledsoe et al. 1988; Kuwabara and Zook 1991; Banks and Smith 1992), periolivary regions (Glendenning et al. 1981; Kuwabara and Zook 1991), and the anteroventral cochlear nucleus (Bledsoe et al. 1988; Winter et al. 1989; Schofield and Cant 1992).

The polymorphic synaptic input onto MNTB principal cells and the manifold efferent projections described above suggest that these neurons play a more diverse role in the ascending auditory pathway than simply being a sign-converting relay station between the VCN and the contralateral LSO. The present study was therefore designed to provide further information about the efferent projections from the MNTB and evaluate possible physiological implications. Until now, there were only very few in vivo studies of the physiology of MNTB neurons in the cat (Guinan et al. 1972a,b; Smith et al. 1989) and none in the rat. The studies in the cat have described a phasic-tonic discharge pattern in response to contralateral acoustic stimulation, similar to the primary-like pattern of auditory nerve fibres. In order to provide more physiological data and also a better understanding of the morphological complexity of MNTB principal cells with respect to the efferent projections, we performed an intracellular in vivo study in the rat. Using microelectrodes filled with horseradish peroxidase (HRP) we analysed the physiology and morphology of individual MNTB principal neurons. By doing so, we were able to reveal their projection pattern at the cellular level and could attribute axonal labelling in target nuclei to a single cell. In addition, the in vivo technique allowed us to circumvent the problems which are necessarily associated with in vitro studies; namely, that the limited thickness of a brain slice enables only a rudimentary or fragmentary reconstruction of the neuronal morphology. A preliminary report of this work has been presented (Sommer et al. 1992).

Materials and methods

Surgical procedure

Twenty-seven adult female Sprague-Dawley rats, weighing 180–250 g, were used in the present study. Care was taken that animals had clean outer ear canals and healthy ear drums. Anaesthesia was induced by intramuscular injections of ketamine (100 mg/kg), xylazine (2 mg/kg) and chlorpromazine (10 mg/kg), and animals were placed in a stereotaxic frame using hollow ear bars. Injections of one quarter of the initial dose were made if required to maintain anaesthesia. Body temperature was kept at 38.5°C and fluid was given subcutaneously at approximately 1-h intervals. After craniotomy, parts of the cerebellar vermis were removed by suction to reveal the floor of the fourth ventricle.

Stimulation procedure

Pure-tone (range 5–55 kHz) or broad-band-noise pulses (range 5–60 kHz) of 80 ms duration with a 2.5 ms rise and fall time were presented at a repetiton rate of 1 Hz. Stimuli were presented via a dichotic stimulation system coupled to the two hollow ear bars. The acoustic system was calibrated in four animals as described previously (Friauf and Ostwald 1988) and loudspeakers (piezoceramic elements) were maximally sensitive between 10 and 55 kHz.

Recording and staining procedure

Recordings were performed on a vibration isolation table. Acoustically driven neurons were penetrated within the superior olivary complex (SOC) and stable recordings from MNTB neurons could be obtained intra-axonally close to their cell bodies. Recording electrodes were glass micropipettes (tip diameter 0.5–1 μm) filled with 9% HRP in 0.1 M TRIS buffer/0.5 M KCl solution (pH 7.6, electrode resistance 30–35 MΩ). Physiological data were stored on FM tape and subsequently analysed. HRP was iontophoretically injected for 1–10 min using 7–12 nA of pulsed depolarising current (pulse duration 500 ms, frequency 1 Hz). To enable the exact correlation of electrophysiological and morphological results, only one cell was injected on each side of the brainstem.

Histological procedure

After a survival time of 8 h under anaesthesia, the animals were perfused transcardially with 0.9% NaCl in 0.01 M phosphate buffer followed by a cold mixture of 1% paraformaldehyde and 2.5% glutaraldehyde in 0.1 M phosphate buffer. Brains were removed and stored overnight in a cold, phosphate-buffered 30% sucrose solution. Frozen sections were cut at 80 μm in the coronal plane and HRP was visualised with diaminobenzidine using slight modifications of the methods of Itoh et al. (1979) and Adams (1981). The sections were then mounted on gelatin-coated slides, counterstained

with thionin, dehydrated and cleared, and finally enclosed with coverslips.

Morphological analysis

Labelled neurons were drawn from the coronal sections with the aid of a camera lucida at a total magnification of $\times 400$–500. Neuronal processes in subsequent sections were drawn in different colours in order to retain depth information. For three-dimensional reconstruction, the x and y coordinates of 700–1200 cell points (e.g. branch points and end points) were digitised and fed into a computer. *Z*-values were obtained by data entry of points located on the surface of a section (80 μm apart) and by algebraic interpolation of values for points within a section. Neurons were reconstructed in two views, a "coronal" and a "horizontal", thereby illustrating the neuronal silhouette. This was achieved by projecting the neuronal morphology onto the coronal or the horizontal plane. The borders of relevant auditory nuclei were determined from the coronal sections and also projected onto the coronal and horizontal plane; they represent the maximal extent of these structures in both types of reconstruction. The overall length of the dendritic trees or the axons was estimated from the x-y-z-coordinates using the pythagorean theorem. For the sake of clarity, drawings were reflected onto the right half of the brainstem when necessary. Measurements of soma and axon diameters were performed at a magnification of $\times 1250$. Two cell body diameters were determined: the longest diameter (D) and the longest diameter (d) perpendicular to D. From these diameters, the soma size A was calculated with the assumption that the soma is an ellipse ($A = D \times d \times \pi/4$).

Electrophysiological analysis

Electrophysiological data were analysed off line. Spike amplitudes were directly measured from voltage traces on the oscilloscope and peristimulus time histograms (PSTHs, 1 ms bin width, ten stimulus presentations) were generated. First-spike latencies were determined from PSTHs with 0.5 ms bin width, considering two action potentials above the spontaneous activity as a suprathreshold response. The rate of spontaneous activity was calculated from 5×200 ms of stimulus-free time.

Results

Electrophysiology

The results presented in the following are based on 11 MNTB neurons that were characterised from intracellular recordings and injections of HRP. All recordings were made from axonal penetrations in the vicinity of the cell body, as was apparent from the disruption of the HRP-labelled axon over a short distance at the recording site (not shown). Due to the axonal recordings, action potentials rather than subthreshold postsynaptic potentials were observed. Stable recordings were difficult to obtain and membrane resting potentials ranged from -10 mV to -30 mV. Although these membrane resting potentials were quite low, they were well within the range reported by others in intracellular in vivo experiments from auditory brainstem neurons (Friauf and Ostwald 1988; Spirou et al. 1990). Intracellular recordings lasted between 2 and 15 min. Because of the limited recording time, neurons were briefly characterised electrophysiologically, HRP was then injected, and the best frequency (BF) was determined. As some neurons were lost during HRP injection, BFs were only determined for six neurons.

All neurons were spontaneously active and the rate of spontaneous discharge ranged from 95–123 spikes/s (mean 109 spikes/s, $n = 6$). Responses to acoustic stimulation of the contralateral ear with noise pulses or pure-tone pulses consisted of spike trains that lasted for the duration of the stimulus (Fig. 1). When stimulus intensities above 60 dB SPL were used, the membrane potential often shifted towards hyperpolarised values during the stimulus pulse and thereafter (Fig. 1). The amount of the shift was intensity dependent and could reach a maximum of 4 mV. Peristimulus time histograms (PSTHs) showed that the characteristic sequence of action potentials was composed of a phasic-tonic discharge pattern (Fig. 2). The amplitude of the phasic component was less pronounced than that described by Guinan et al. (1972a, Fig. 5, category B), and a brief, profound dip between the initial peak and the tonic phase was also not observed. It should, however, be mentioned here that we generated our PSTHs with only ten stimulus presentations, and it is therefore conceivable that we may have missed the dip. Consequently, we are unable to decide whether the response pattern of the recorded MNTB neurons was the same (i.e. primary-like with notch) as that of their input neurons (globular bushy cells in the contralateral VCN). The firing threshold as determined with noise pulses ranged between 30 and 60 dB SPL. After stimulus offset, the spontaneous activity was decreased in all neurons and often completely suppressed for about 10 ms (Figs. 1, 2). Suppression of the spontaneous activity lasted a maximum of 21 ms. Increasing the stimulus intensity increased the neurons' firing rate in a linear fashion (not shown). Since the neurons' discharge rate increased linearly up to a stimulus intensity of 80 dB SPL (our maximal intensity), it remains unclear whether their rate-intensity function was monotonic. The first-spike latency was determined 30 dB SPL above firing threshold and ranged from 3.3 to 3.9 ms (mean 3.5 ms, $n = 6$). The neurons' BFs ranged from 14 to 47 kHz ($n = 6$) and were thus within the rat's hearing range (0.7–60 kHz at 40 dB SPL) that was determined in behavioural studies (Kelly and Masterton 1977). The fact that BFs below 14 kHz were not observed may be explained by the high-frequency type of piezo-loudspeaker used (see Materials and methods).

Soma-dendritic morphology

All somata ($n = 11$) were found in the MNTB (Fig. 3) and were distributed throughout most of its rostrocaudal length, with the majority clustered in the medial third (Table 1). Somata were globular or oval and the mean cell body diameters D and d were 21.9 μm (range 15–30 μm) and 14.3 μm (range 10–20 μm), respectively. This resulted in a mean soma size (for an ellipse) of 246.0 μm^2 (range 153–393 μm^2). Because of their somatic characteristics as well as the presence of one or two primary, slender dendrites emerging from the somata (Figs. 3, 4), the MNTB

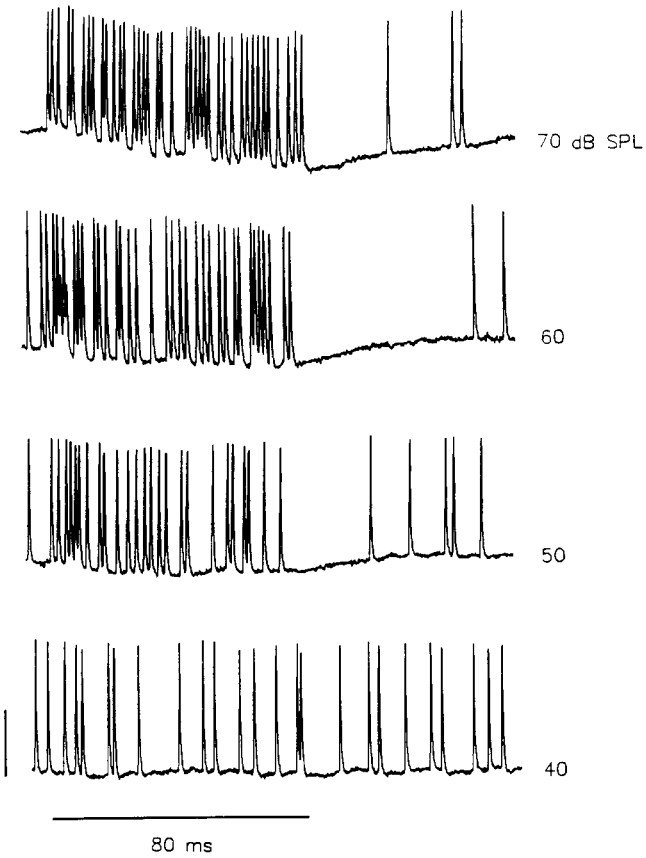

Fig. 1. Intra-axonal recordings from a neuron in the MNTB following acoustic stimulation of the contralateral ear with broad-band noise pulses (80 ms duration) between 40 and 70 dB SPL. Note the characteristic sequence of stimulus-elicited action potentials, which is composed of a tonic discharge pattern followed by a transient inhibition of the spontaneous activity after stimulus offset. Also note that the membrane potential becomes hyperpolarised during the stimulus presentation and thereafter, and that the effect depends on stimulus intensity. *Vertical bar* 5 mV. Best frequency (BF) 36 kHz

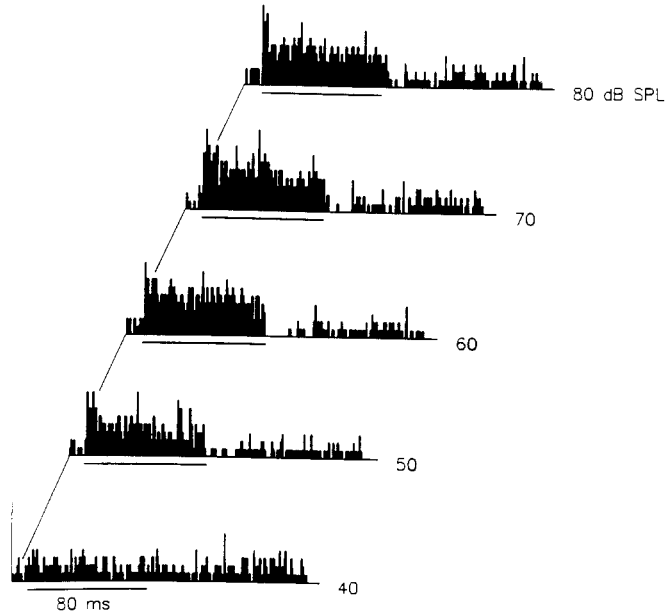

Fig. 2. Characteristic peristimulus time histograms (PSTHs) of an MNTB neuron following stimulation of the contralateral ear with tone pulses (80 ms duration) of 40–80 dB SPL at the neuron's BF (15 kHz, ten stimulus presentations per PSTH, 1 ms bin width). The firing threshold of this neuron was slightly above 40 dB SPL. A phasic-tonic discharge pattern and the transient inhibition of the spontaneous activity after tone offset become obvious. *Vertical bar* 10 spikes

neurons could be identified as principal cells. This is consistent with previous descriptions (Ollo and Schwartz 1979; Kuwabara and Zook 1991; Banks and Smith 1992). If two primary dendrites were present, they often originated from opposite poles of the soma, thus giving the neurons a bipolar appearance (Fig. 4). A few primary dendrites remained unbranched, with the majority branching repetitively, giving off daughter branches of secondary and tertiary order; occasionally, dendrites of 5th–7th order were seen (Fig. 4). Dendritic branches were spineless, as was also observed by Banks and Smith (1992). This feature may be species-specific, since spines have been observed on MNTB principal cells of other species (cat, Morest 1968; big brown bat, moustache bat, mouse, gerbil, Kuwabara and Zook 1991). Dendrites were mainly oriented horizontally, often extending beyond the nuclear boundary into the trapezoid body and continuing towards the midline (Figs. 4, 6, 10). The average total length of the dendritic arbors, as estimated by the Pythagorean theorem, was 1063 µm. Compared with the size of dendritic arbors of facial motoneurons (17650 µm, Friauf 1986), trigeminal motoneurons (25000 µm, Lingenhöhl and Friauf 1991), and neurons in the reticular formation (17700 µm, Lingenhöhl and Friauf 1992), the dendritic trees of MNTB principal cells are remarkably small. This indicates that the postsynaptic surface for afferent input, which is formed by the dendrites, plays a relatively insignificant role in these neurons, consistent with the assumption that the major afferent input comes from the calyces of Held and that other synaptic contacts play a modulatory role. However, as HRP injections were made intraxonally, distal dendrites were mostly weakly labelled, and it is thus possible that we did not completely reveal the whole dendritic arbors and therefore underestimated the overall dendritic length.

Axonal morphology

Main axon. The axonal course of ten neurons was reconstructed and forms the basis of our morphological analysis. The intra-axonal injection of HRP allowed for intensive labelling of the main axon and the axonal trajectory could thus be followed over a considerable distance from the soma. Even distal axon collaterals were darkly labelled (Fig. 5), and therefore it is likely that the complete axonal morphology was demonstrated in most neurons. Examples of three HRP-injected neurons are illustrated in Figs. 6–9. All axons emerged directly from the soma, mostly ($n=9$) from its dorsal or dorsomedial side and only in two cases from the lateral side. Axons that initially coursed medially changed their direction within the nuclear domain of the MNTB and projected dorsally and/or laterally into the SPN and the LSO. Projections to the contralateral side of the brainstem were never ob-

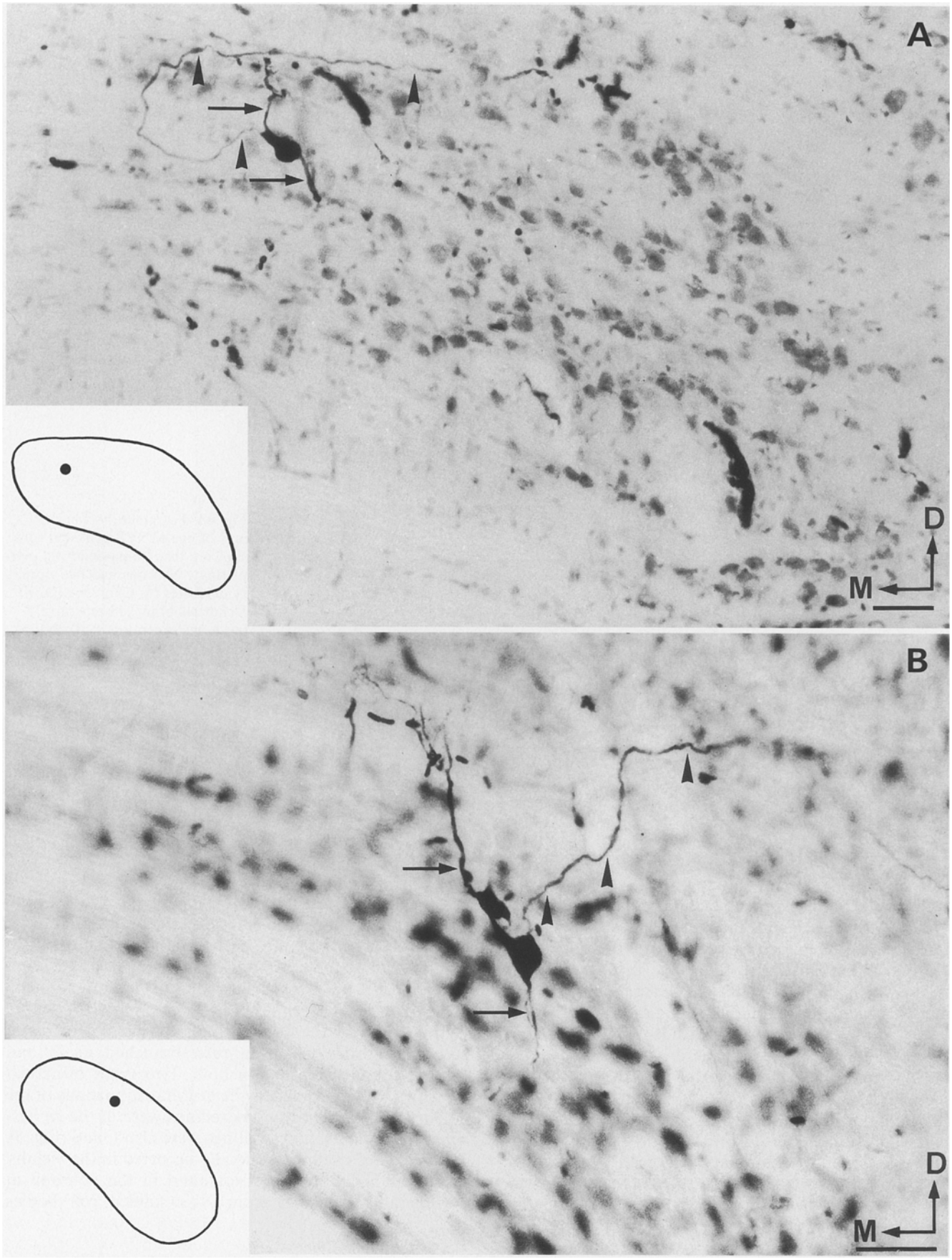

Fig. 3A,B. Photomicrographs of two HRP-injected MNTB neurons in coronal sections through the brainstem. Note the oval shape of the somata, the two primary dendrites per neuron which emerge from opposite poles of the soma (*arrows*), and the main course of the proximal axon which extends laterally (*arrowheads*). Based on these morphological properties, neurons were identified as MNTB principal cells. *Insets* show location of the cell bodies within the MNTB. The BF of the neuron in **A** was 38 kHz. *D*, Dorsal; *M*, medial. *Bars* 50 μm

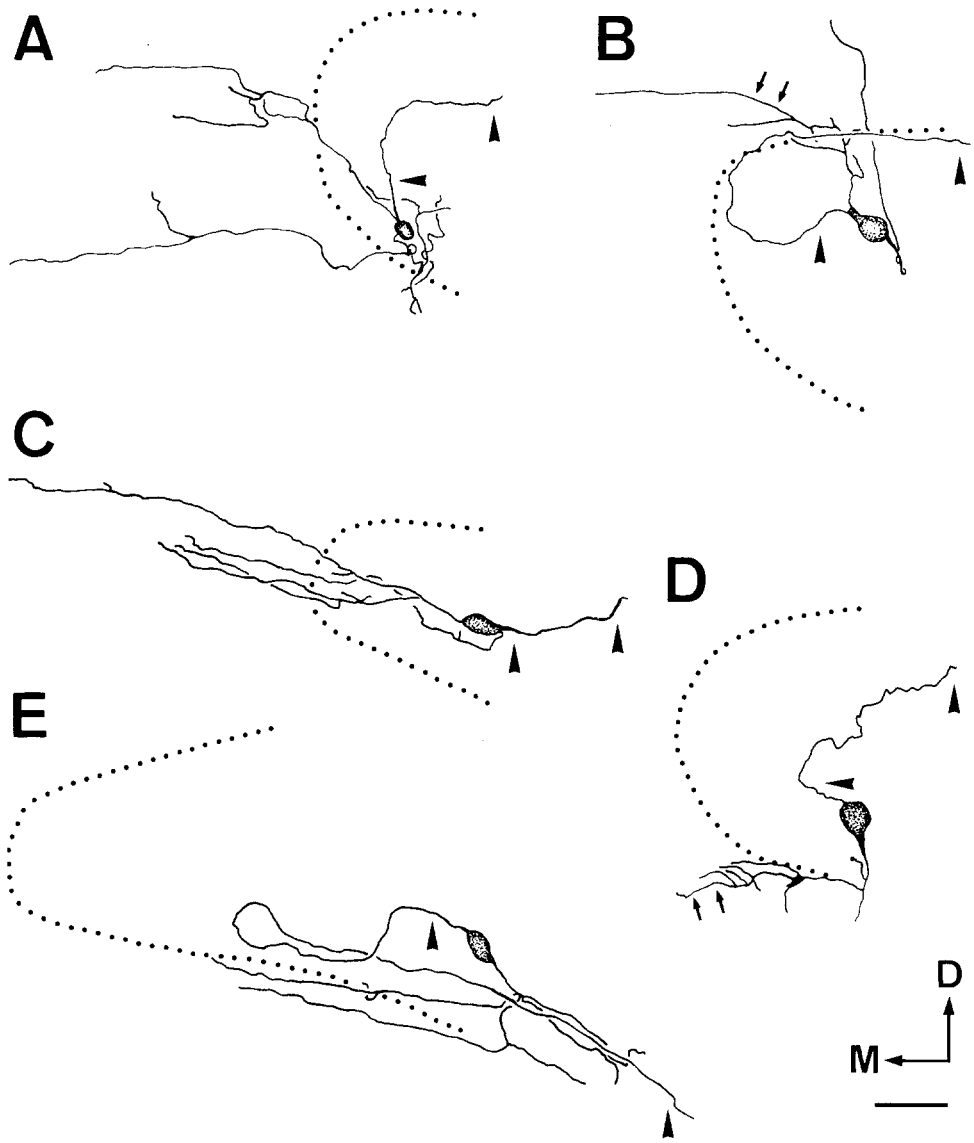

Fig. 4A–F. Camera-lucida drawings of five MNTB principal cells showing their soma-dendritic morphology. Neurons had two primary dendrites (**A–C**) or one (**D, E**). Dendrites branched repetitively (note one exception in **B**) and extended beyond the boundary of the MNTB (dotted lines). Occasionally, dendritic branches of fifth to seventh order were seen (*arrows* in **B, D**). *Arrowheads* depict axons, which generally ran dorsolaterally. Available BFs for the neurons were 47 kHz (**A**), 38 kHz (**B**), and 36 kHz (**D**). *D*, Dorsal; *M*, medial. *Bar* 50 μm

served. The axons from nine of ten principal cells projected beyond the LSO and entered the lateral lemniscus where they ascended further dorsally and rostrally, often more than 2 mm rostral to the soma. In the remaining case, for which a projection into the lateral lemniscus was not clearly identified, axonal labelling in the lateral lemniscus was present, but we could not unequivocally attribute it to the injected cell. Thus, it is quite possible that all MNTB principal cells projected into the lateral lemniscus. The mean axon diameter was determined at various sites along the axonal course. Close to the soma it was 1.6 μm (range 1.3–2.0 μm), and it did not change significantly upon reaching the LSO (mean 1.7 μm; range 1.2–2.0 μm). However, distal to the LSO the axons tapered, and shortly before entering into the lateral lemniscus, their diameter had decreased to 1.25 μm (range 1.0–1.4 μm). This indicates that the projection to the NLL is not made by the main axon with a thick diameter and consequently a high conduction velocity, but rather by an axon collateral with lower conduction velocity.

Axon collaterals and terminal endings. The axons of the MNTB principal neurons branched heavily and gave off collaterals at various sites in the brainstem. The average length of an axon, including all collaterals, was 15.7 mm (range 12.5–17.8 mm). Projections to several auditory target nuclei were seen (Table 1). These projections were characterised by the formation of multiple collaterals of secondary order which in turn branched again and formed complex terminal arbors. Two types of axonal swellings were observed at the distalmost portions of the collaterals: the majority of swellings were of the *en passant* type, but terminal swellings were also found (Fig. 5). Both types of swellings generally occurred in the vicinity of cell bodies, but were also found in the neuropil at considerable distances from Nissl-stained cell bodies (Fig. 5).

Target nuclei

All ten reconstructed MNTB principal neurons had axon collaterals that terminated in the LSO and in the SPN (cf.

Table 1. Characteristics of HRP-injected MNTB principal cells

Unit	BF (kHz)	Rostro-caudal location of cell body in MNTB[a] (%)	Projections into										Number of auditory targets
			LSO	Rostro-caudal extent of terminal arbor in LSO (μm)	SPN	Rostro-caudal extent of terminal arbor in SPN (μm)	MSO	LNTB	Peri-olivary regions	VNLL	DNLL	AVCN	
1	14	38	+	320	+	400	−	−	?	?	?	−	2
2	15	46	+	320	+	480	−	+	+	?	?	−	4
3	30	59	+	160	+	640	−	+	+	?	?	−	4
4	38	54	+	320	+	1040	−	−	+	?	?	−	3
5	47	35	+	240	+	1200	−	−	+	+	?	−	4
6	?	24	+	320	+	400	−	−	+	?	?	−	3
7	?	57	+	400	+	720	−	−	+	?	?	?	3
8	?	69	+	480	+	800	−	+	+	?	?	−	4
9	?	56	+	320	+	400	−	+	+	?	?	−	4
10	?	47	+	640	+	880	+	+	+	+	+	−	7
Sum			11		11		1	5	9	2	1	?	

AVCN, Anteroventral cochlear nucleus; *DNLL*, dorsal nucleus of lateral lemniscus; *LNTB*, lateral nucleus of trapezoid body; *LSD*, lateral superior olive; *MNTB*, medial nucleus of trapezoid body; *MSD*, medial superior olive; *VNLL*, ventral nucleus of lateral lemniscus
[a] 0% and 100% correspond to the caudalmost and rostralmost sections though the MNTB, respectively

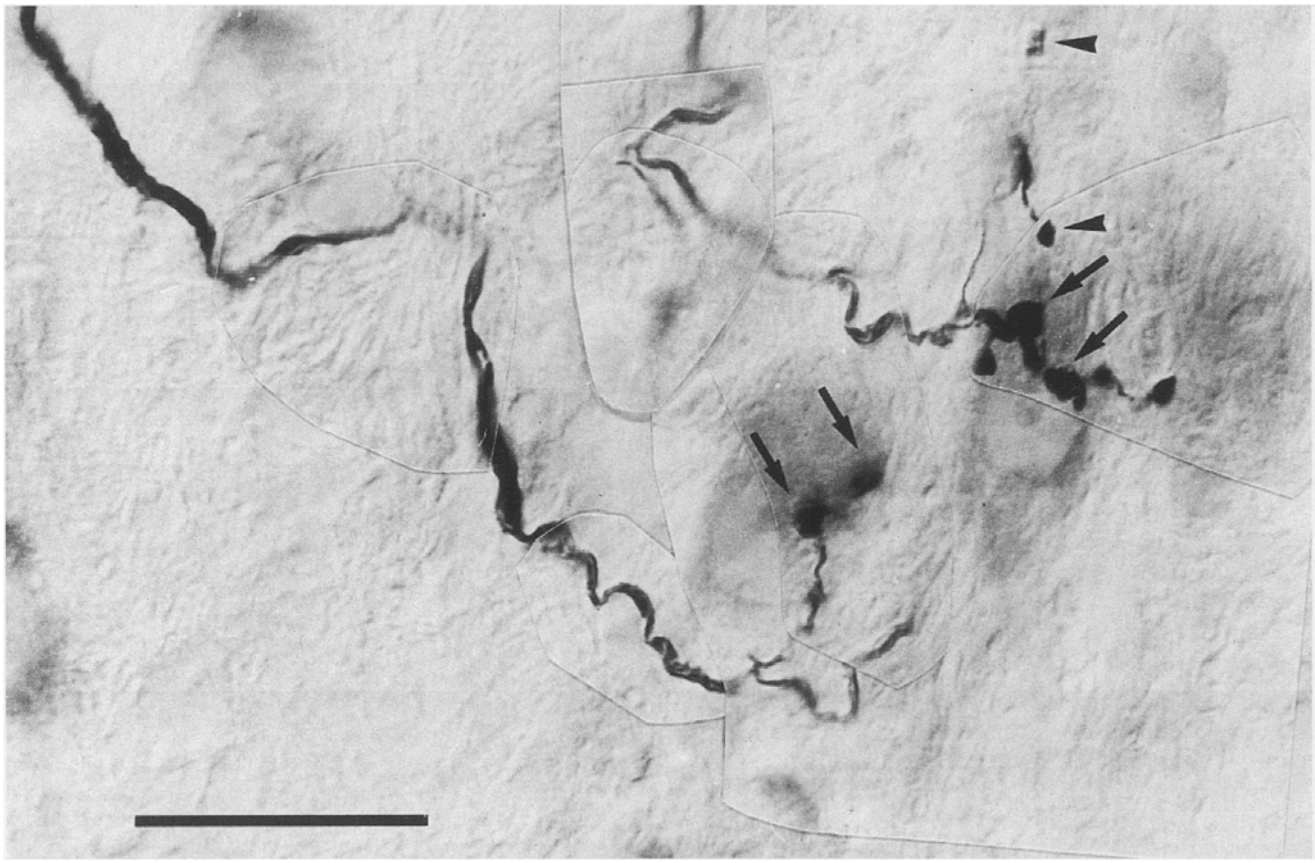

Fig. 5. High magnification photomicrograph of terminal axonal collaterals of an MNTB principal cell in the center of the LSO. Boutons en passant (*arrows*) and boutons terminaux (*arrowheads*) are present, terminating in close proximity to Nissl-stained cell bodies or within the neuropil. Dorsal is to the top, lateral to the right. *Bar* 25 μm

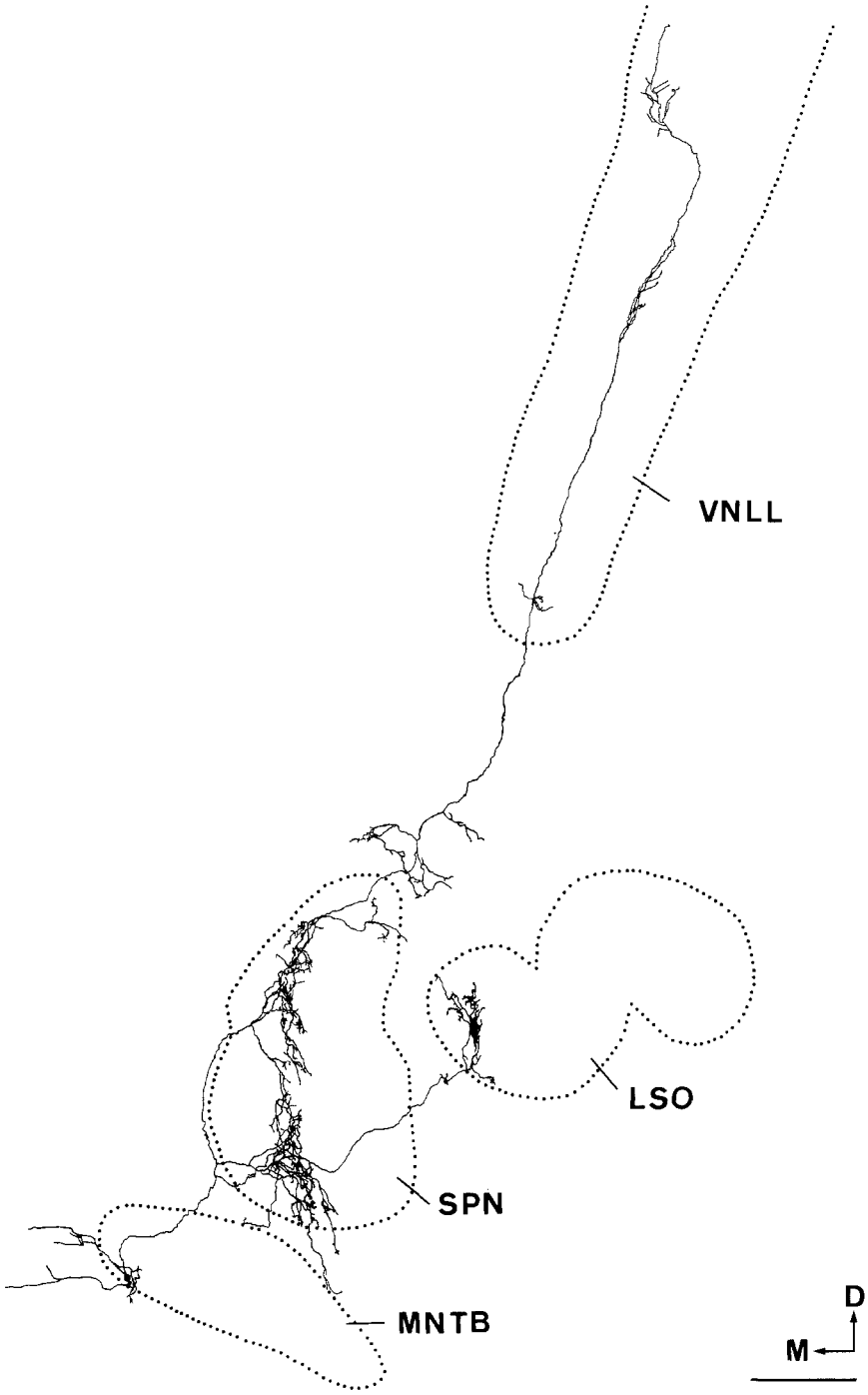

Fig. 6. Camera-lucida drawing of an MNTB principal cell (unit 5, BF 47 kHz), illustrating its axonal trajectory and termination pattern in a 'coronal' view (see Materials and methods for explanation). The axon, which appears to be completely filled, branches heavily and has terminal arborisations in four auditory brainstem areas: the lateral superior olive (*LSO*), the superior paraolivary nucleus (*SPN*), the ventral nucleus of the lateral lemniscus (*VNLL*), and periolivary regions. Note the location of the cell body and the axonal terminals in medial aspects of the MNTB and LSO, respectively. Dendrites extend medially and reach beyond the nuclear boundary into the trapezoid body. *D*, Dorsal; *M*, medial. *Bar* 250 μm

Figs. 6–9). In addition, nine neurons projected to areas within the SOC which could not be attributed to a nucleus proper; these collaterals were therefore regarded as collaterals within periolivary regions. Apart from the obligatory target nuclei (i.e. the LSO and SPN), terminal axonal arbors could be unequivocally identified in four other auditory nuclei: the LNTB, the VNLL, the DNLL, and the MSO. Thus, as a population, MNTB principal cells projected to at least seven different auditory nuclei and also into periolivary regions. Individual MNTB principal cells could innervate between two and seven auditory targets (Table 1). Projections into the LNTB were observed in five of ten neurons (cf. Figs. 7, 8), projections into the VNLL in two neurons (cf. Figs. 6–8), and projections into the DNLL and the MSO in only one neuron (cf. Figs. 7, 8). One neuron was identified as giving rise to a long axon with a collateral projecting towards the cochlear nucleus (Fig. 9). Unfortunately, the HRP reaction product became invisible shortly ventromedially to the anteroventral cochlear nucleus (AVCN), and it therefore remains unclear whether this neuron did in fact project into the AVCN or even into the cochlea.

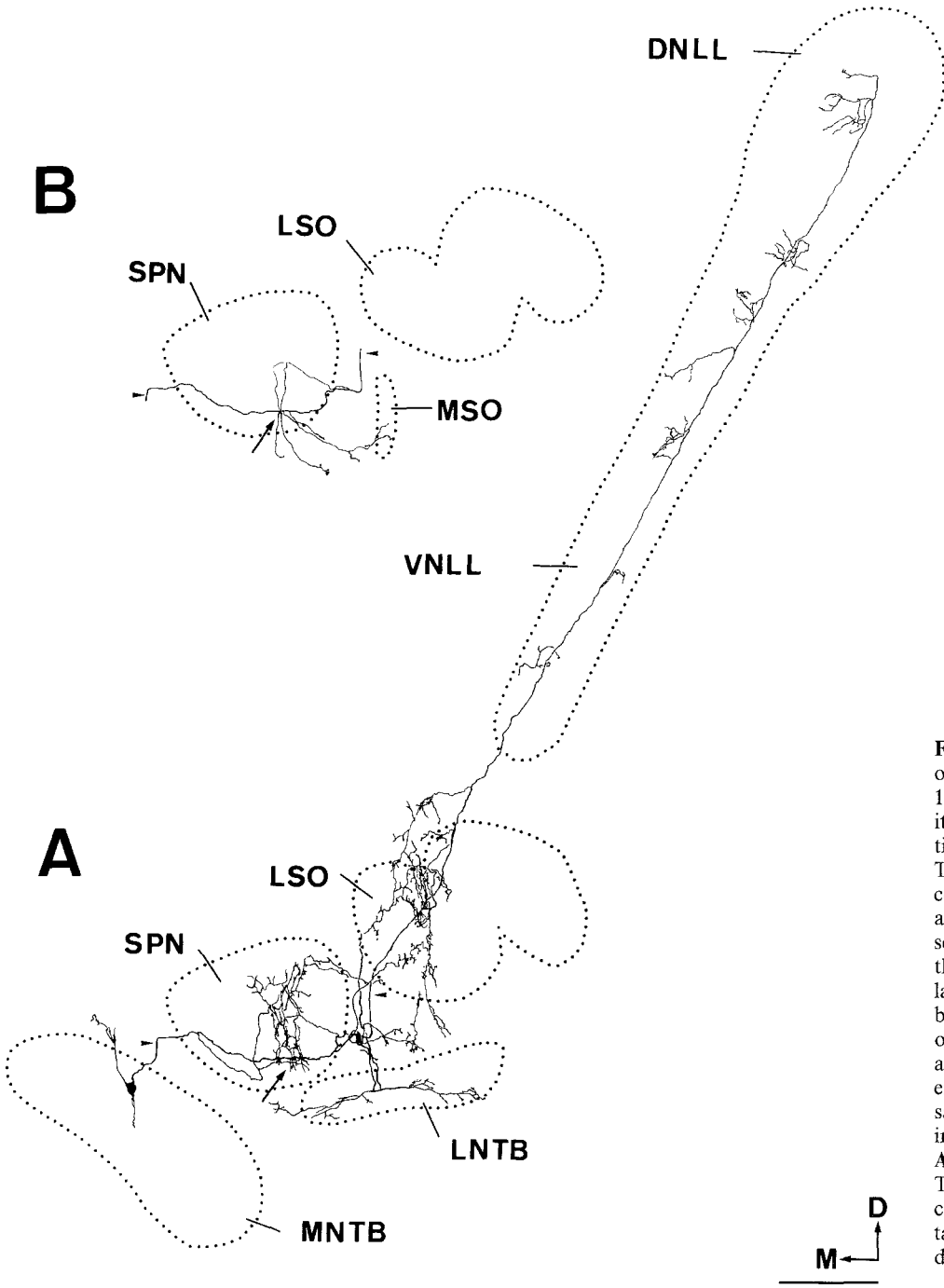

Fig. 7A,B. Camera-lucida drawing of an MNTB principal cell (unit 10, no BF available), illustrating its axonal trajectory and termination pattern in a 'coronal' view. The axon, which was probably completely filled, branches heavily and has terminal arborisations in seven auditory brainstem areas: the LSO, the SPN, the VNLL, the lateral nucleus of the trapezoid body (*LNTB*), the medial superior olive (*MSO*), periolivary regions, and the dorsal nucleus of the lateral lemniscus (*DNLL*). For the sake of clarity, the terminal arbors in the MSO are not illustrated in **A**, but are shown separately in **B**. The *arrows* point to the site of collateralisation; *arrowheads* facilitate matching. *D*, Dorsal; *M*, medial. Bar = 250 μm

Tonotopic organisation of the projections

As already seen in Figs. 6–9, a restricted extent of the axonal arbors in the LSO and the SPN was often observed. Within these nuclei, the terminal axonal fields were oriented dorsoventrally and restricted mediolaterally, indicating that the afferent MNTB projections were topographically organised, following a mediolateral gradient. The projections into the LSO are summarised for five MNTB principal cells with known BFs in Fig. 10. Neurons with high BFs projected into medial aspects of the LSO, whereas those with lower BFs projected further laterally, consistent with the tonotopic axis in the LSO which runs from the medial to the lateral limb with decreasing frequency. A similar situation was observed in the SPN, despite the fact that the axonal arbors were less confined in this nucleus (Fig. 11). MNTB neurons with higher BFs projected to aspects of the SPN further medial than those supplied by neurons with lower BFs, suggesting that the SPN is tonotopically organised and that the tonotopic axis is directed like that in the LSO (from lateral to medial with increasing frequency). Projections into the VNLL were generally characterised by several, spatially separated, terminal fields, each running horizontally within the nucleus (Figs. 6, 7). However, because of the limited number of neurons with clearly identified projections into the VNLL ($n=2$) in our sample, we were not able to correlate the location of the horizontal bands

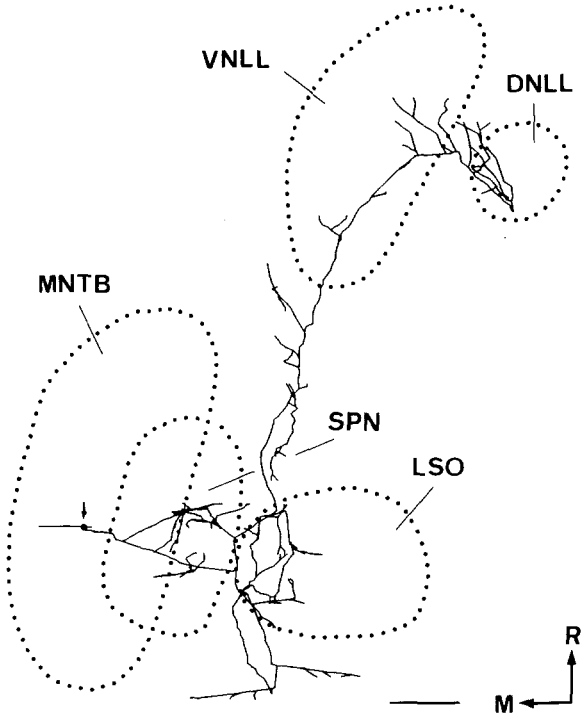

Fig. 8. Computer reconstruction of the neuron shown in Fig. 7 (based on 829 cell points) to illustrate the extent of its axonal trajectory as seen in a 'coronal' view. *Small arrow* points to the cell body. For the sake of clarity, the nuclear boundaries of the MSO and the LNTB are not shown. Note that the rostrocaudal width of the axon is almost 2.5 mm. *M*, medial; *R*, rostral. *Bar* 250 μm

with the BF, with the same argument holding for the MSO and the DNLL. Nevertheless, our data provide clear evidence against a tonotopic organisation of the LNTB, as the terminal axon arbors in this nucleus extended over large areas in all directions (cf. Fig. 7).

Aside from the extent of the axonal arbors in the coronal plane, the extent in the rostrocaudal dimension of the LSO and the SPN was also calculated for each cell. To do so, the number of serial coronal sections that contained labelled axon terminals and/or nuclear territory were counted. None of the axonal arbors of MNTB principal cells extended throughout the whole nucleus. Axonal arbors were restricted to 160–640 μm (corresponding to 29–89%) of the LSO's rostrocaudal thickness (cf. Fig. 8, Table 1). In the SPN, axonal arbors extended over greater distances and occupied 400–1200 μm (corresponding to 34–93%) of the nuclear rostrocaudal thickness. Despite the limited extent in the rostrocaudal dimension, the majority of many arbors exceeded 500 μm, i.e. greater than the thickness of most brainstem slices, thereby clearly illustrating the limitations of the slice technique in completely revealing the anatomy of individual neurons – even if the technique is concentrated on intrinsic connectivity – such as that within the SOC. The high variability in the size of our axonal arbors in the rostrocaudal dimension did not correlate with the labelling intensity, because the most intensely labelled neurons did not have the longest axonal arbors. The location of the axonal arbors within the target nuclei varied; axonal arbors

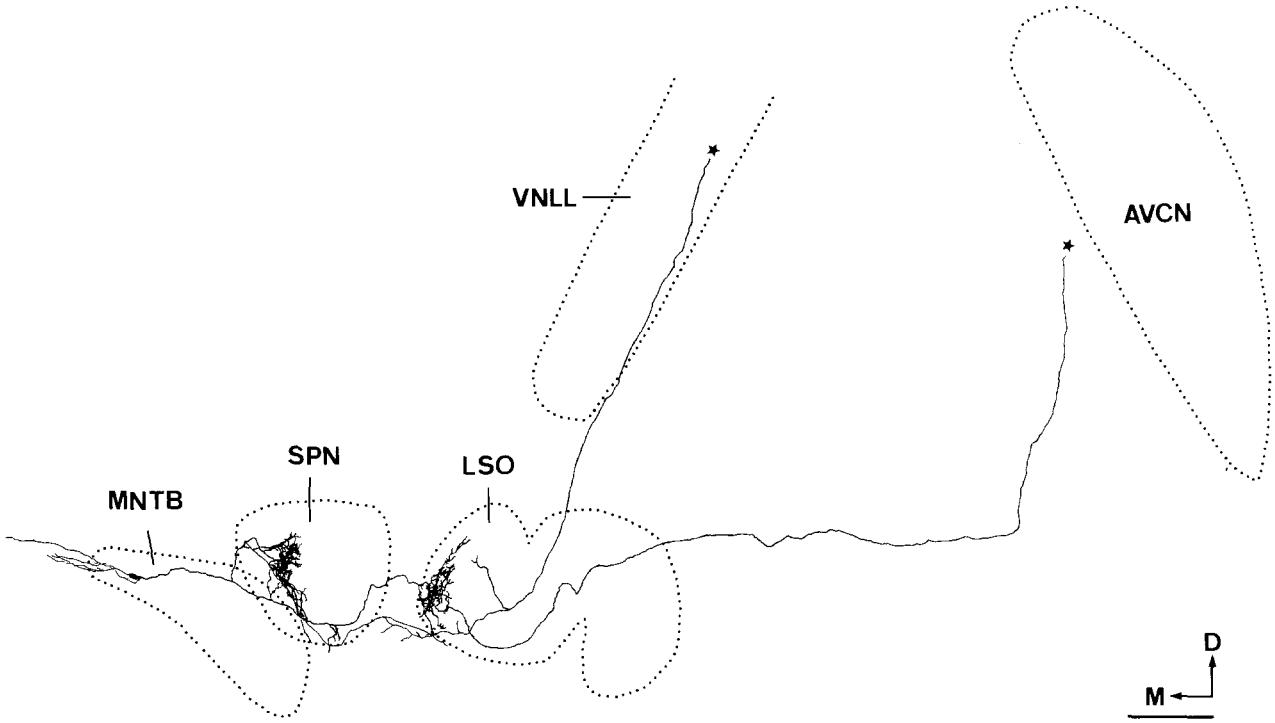

Fig. 9. Camera-lucida drawing of an MNTB principal cell (unit 7, no BF available), illustrating its axonal trajectory and termination pattern in a 'coronal' view. The axon was incompletely filled and the two sites where the HRP reaction product became invisible are marked by *stars*. The axon branches heavily and has terminal arborisations in the LSO, the SPN, and in periolivary regions. In addition, there are two long axon collaterals, one projecting into the VNLL and another one immediately medial to the anteroventral cochlear nucleus (*AVCN*) (the rostrocaudal width of the axon was about 2 mm, not shown). An axonal projection towards the AVCN was not seen in any other labelled MNTB neuron. Dendrites extend medially and reach beyond the nuclear boundary, terminating in the trapezoid body. *D*, Dorsal; *M*, medial. *Bar* 250 μm

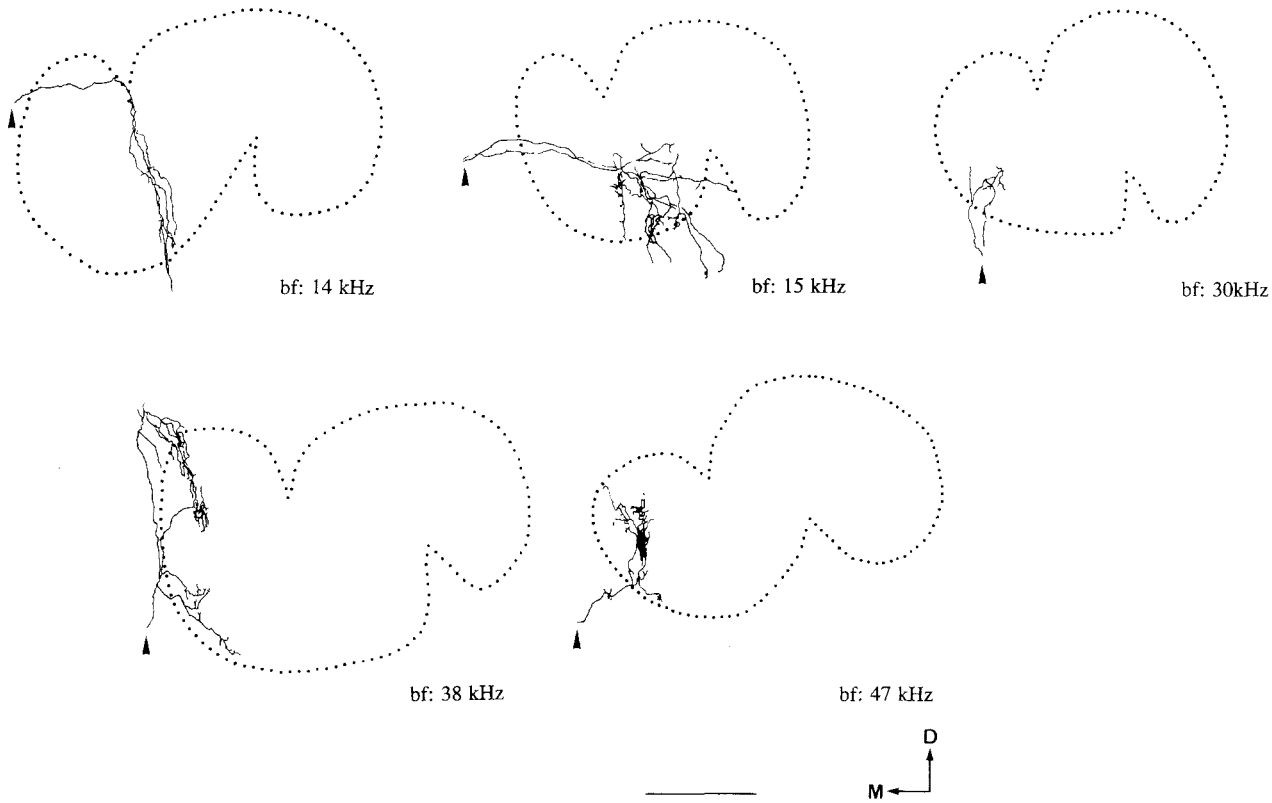

Fig. 10. Topographic relationship between the BF of five MNTB principal cells and the position of their terminal axonal arbors in the LSO. With increasing BF, the position of the terminal arbors shifts from lateral towards medial, indicating that the tonotopic axis from low to high runs from lateral to medial. *D*, Dorsal; *M*, medial. *Bar* 250 μm

could be restricted to the caudal third of the LSO (not shown) or extend throughout most of its rostrocaudal extent (Fig. 8). Furthermore, axonal arbors that were restricted to about 50% of the SPN's rostrocaudal extent were found in the caudal as well as in the rostral half of the nucleus.

Tonotopic organisation of the MNTB

The location of the cell bodies in the MNTB correlated with the neurons' BFs. As shown in Fig. 12, there was a tonotopic gradient running from medial to lateral when frequencies changed from high to low. Some calyces of Held from globular bushy cells were labelled by intra-axonal HRP injections during the course of our experiments. Their location is also illustrated in Fig. 12 (some data were taken from Friauf and Ostwald 1988). There was a close correlation between the location of the calyces and the BFs, as well as a good correspondence with the tonotopic organisation of MNTB somata.

Discussion

The major result of the present study is the demonstration of multiple target nuclei within and outside the SOC that receive projections from individual MNTB principal neurons (Table 1, Fig. 13). The projection pattern of single MNTB neurons has previously been described in in vitro studies using brainstem slices (Zook and DiCaprio 1988; Kuwabara and Zook 1991; Banks and Smith 1992), but these studies did not reveal the complete axonal morphology of the neurons due to the limited thickness of the brainstem sections. Therefore, except for a recent abstract report on a study performed in the cat (Smith et al. 1989), the present in vivo study is the first detailed report of MNTB projections at the cellular level. Although we could not reveal the complete morphology of all neurons, our data demonstrate the three-dimensional extent of MNTB principal cells in a hitherto undescribed complexity.

Projections to target nuclei

Although our MNTB principal cells were quite homogeneous in their soma-dendritic properties, they appeared to be heterogeneous in their projection pattern. Each reconstructed neuron projected into the LSO and the SPN, whereas projections to other target nuclei, which are intrinsic and extrinsic to the SOC, were only observed in subsets of these cells. The intrinsic SOC projections to the MSO, LNTB and periolivary regions which we observed have also been seen in in vitro experiments (Zook and DiCaprio 1988; Kuwabara and Zook 1991; Banks and Smith 1992). Our results confirm these previous reports, but also demonstrate extrinsic projections to the VNLL and the DNLL (and possibly the AVCN) which originat-

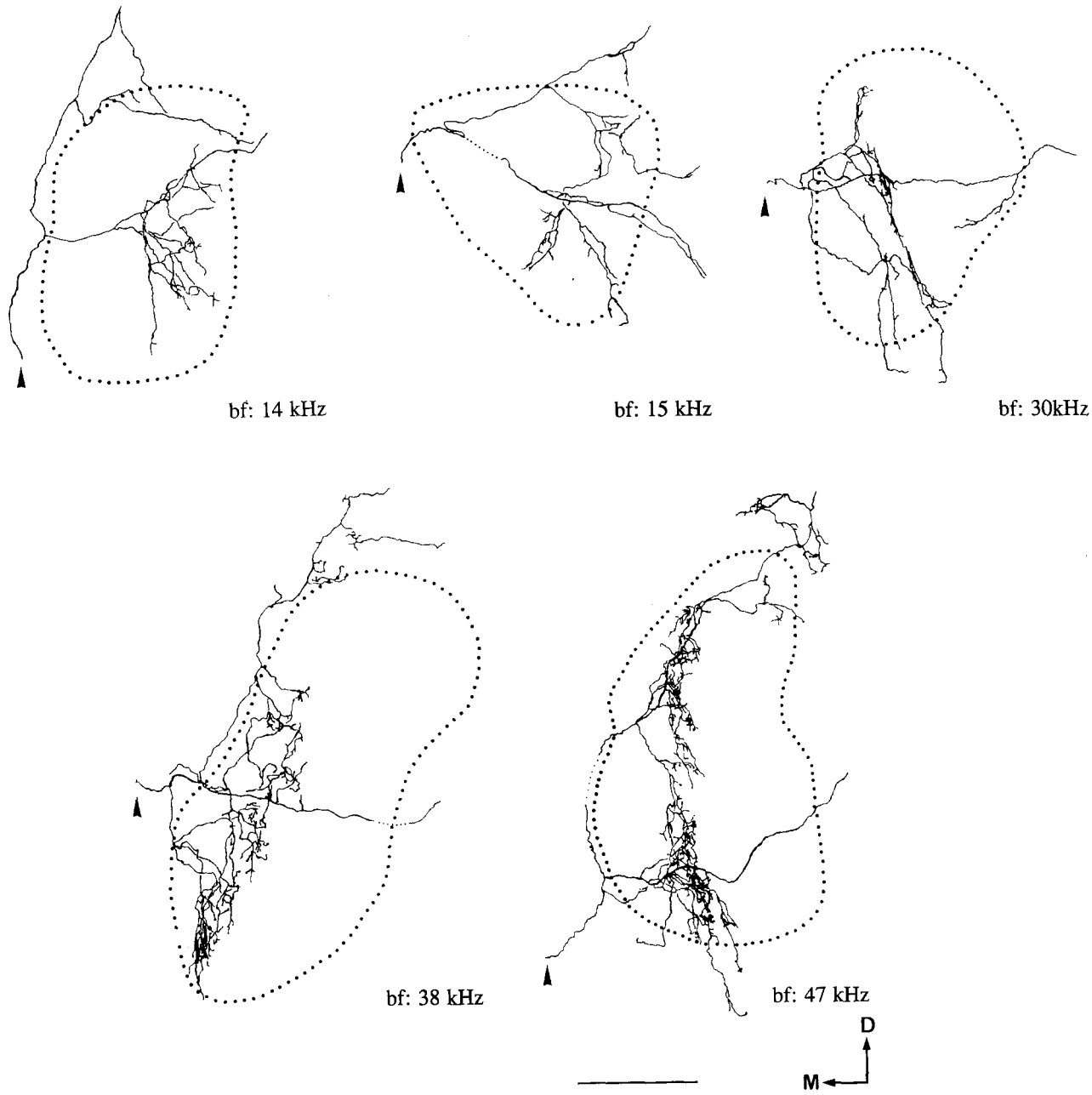

Fig. 11. Topographic relationship between the BF of five MNTB principal cells and the position of their terminal axonal arbors in the SPN. With increasing BF, the positions of the terminal arbors tend to shift from lateral towards medial, indicating that the tonotopic axis from low to high runs from lateral to medial, like that in the LSO, but less distinct (cf. patterns at 38 kHz and 47 kHz). *D*, Dorsal; *M*, medial. *Bar* 250 μm

ed from the same cells. Projections to the nuclei of the lateral lemniscus had been described in cats (Glendenning et al. 1981; Spangler et al. 1985) and guinea pigs (Bledsoe et al. 1988), but it was unknown whether they were made by MNTB principal cells that also had intrinsic SOC projections.

Concerning the identified target nuclei of MNTB principal cells, there is total agreement between the results of the present study and previous reports (see Introduction for references). Thus, although our sample size was small, we feel safe to conclude that it provides a representative analysis of the morphology of individual MNTB principal cells. Slight discrepancies between the results of the present study and previous reports (e.g. Kuwabara and Zook 1991; Banks and Smith 1992) are mainly based on quantitative data. Nevertheless, these discrepancies do not confound our major results and can probably be attributed to the small sample size. A greater number of MNTB neurons with completely reconstructed morphology is necessary for clarification.

Kuwabara and Zook (1991) reported that the somata of those of their MNTB principal cells which projected into the lateral lemniscus tended to be clustered in the rostral half of the MNTB. Our data do not confirm this

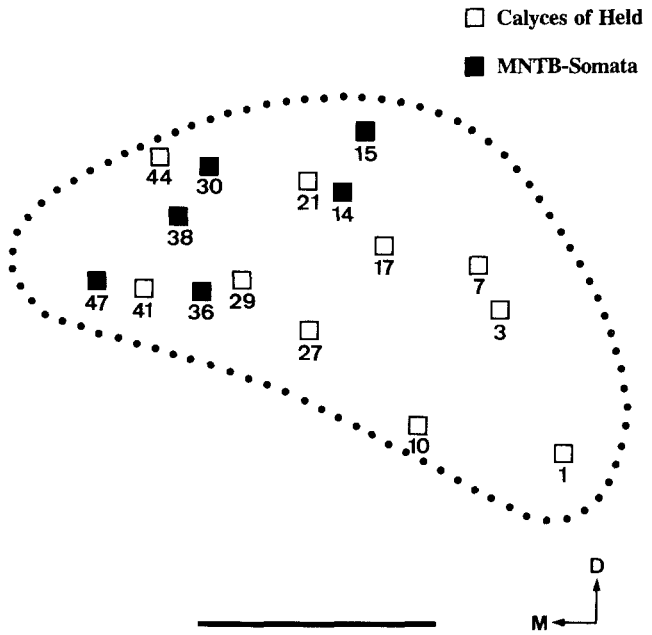

Fig. 12. Tonotopic organisation of the rat MNTB. The diagram illustrates the position of the cell bodies from six MNTB principal cells (*filled squares*) and the position of ten calyces of Held from globular bushy cells from the contralateral cochlear nucleus (*open squares*). Data from the present study (21, 29, 41, and 44 kHz) and from Friauf and Ostwald [(1988) 1, 3, 7, 10, 17, and 27 kHz]. BFs are demonstrated by *numbers* next to the cell body or the calyx and are given in kHz. Note that the unit with a BF of 36 kHz is not included in Table 1, since its axonal morphology could not be reconstructed. The tonotopic axis from low to high runs from lateral to medial in the MNTB. *D*, Dorsal; *M*, medial. *Bar*, 250 μm

conclusion, as most of our cell bodies were located in the middle of the MNTB, and we also found a cell with a lateral lemniscus projection (unit 6) which was located in the caudal quarter (Table 1).

A small group of MNTB principal cells (eight of over 100 cells analysed in four species) has been reported to have recurrent axon collaterals to the originating MNTB (Kuwabara and Zook 1991). However, recurrent collaterals were observed neither by Banks and Smith (1992) nor in the present study. As our injections were made in the vicinity of the cell bodies, i.e. near the point of origin of the recurrent axon collaterals, it is unlikely that we could have missed them. Instead, it is probable that our population ($n = 10$) was too small to identify recurrent collaterals.

We found one MNTB principal cell with a long descending axon collateral which projected toward the ipsilateral AVCN and became invisible near the medial border of the nucleus. The target of this axon collateral remains, therefore, unidentified. It is possible that it terminated in the AVCN, as MNTB-AVCN projections have been described in rodents (guinea pig, Bledsoe et al. 1988; Winter et al. 1989; rat, A. Klepper, personal communication). Winter et al. (1989) also reported descending projections from the MNTB to the cochlea; however, these projections were minor and were not seen in the rat (White and Warr 1983; Aschoff and Ostwald 1987). Thus, it is highly unlikely that the observed collateral descended beyond the cochlear nucleus.

We were able to unequivocally identify seven auditory brainstem areas as the targets of MNTB principal cells

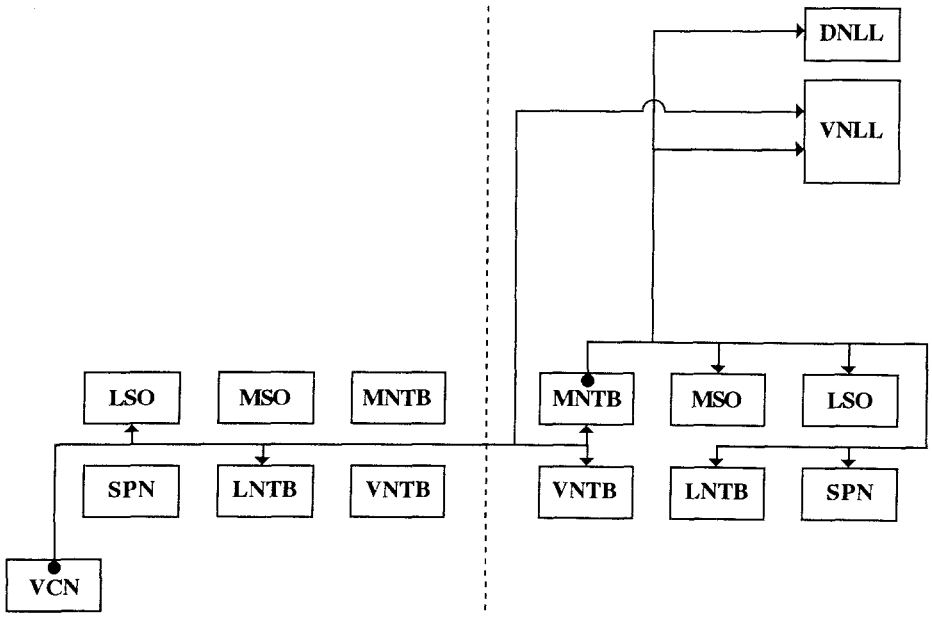

Fig. 13. Schematic diagram illustrating a hypothetical microcircuit in the rat auditory brainstem which may be formed by a single globular bushy cell in the contralateral VCN and a single principal cell in the MNTB. The *broken line* marks the midline, *filled circles* mark the cell bodies, and *arrows* mark projections to target nuclei. Projections to periolivary regions are not shown. Data from the present study and from Friauf and Ostwald (1988). According to the scheme, all illustrated SOC nuclei receive input from the contralateral VCN, either monosynaptically (i.e. directly from globular bushy neurons) or disynaptically (i.e. via MNTB principal cells). Furthermore, VNLL neurons may be exposed to "feedforward inhibition", because they receive excitatory input from globular bushy cells in the contralateral VCN (as do MNTB cells) and inhibitory input from MNTB principal cells. *DNLL*, Dorsal nucleus of lateral lemniscus; *LNTB*, lateral nucleus of trapezoid body; *LSO*, lateral superior olive; *MNTB*, medial nucleus of trapezoid body; *MSO*, medial superior olive; *SPN*, superior paraolivary nucleus; *VCN*, ventral cochlear nucleus; *VNLL*, ventral nucleus of lateral lemniscus; *VNTB*, ventral nucleus of trapezoid body

(LSO, SPN, MSO, LNTB, periolivary regions, VNLL, DNLL). If one includes the AVCN as a potential target, eight auditory target areas receive input from MNTB principal cells. Since our morphological reconstructions were made conservatively and since our population is likely to comprise a subpopulation of all MNTB principal cells (e.g. we found no recurrent axon collaterals), our results are even likely to underestimate the number of all target areas of MNTB principal cells. Seven of the above-mentioned auditory targets were shown to be the possible target of a single cell. Thus our results demonstrate more target nuclei of single MNTB principal cells than were previously described for any mammalian species. This is in clear contrast to the findings by Banks and Smith (1992), who reported that "MNTB cells in the rat appear to have more restricted targets than in other species studied". Again, the discrepancy may be attributed to the different techniques employed, and it again shows that morphological studies in a brain slice preparation, which may be suitable for analysing intrinsic connectivity, most probably fail to sufficiently describe distant projections in all three dimensions.

Tonotopic organisation of the projections

Electrophysiological studies in the cat (Guinan et al. 1972a,b) provided the first evidence of tonotopic organisation of several nuclei in the SOC, with the BFs of units in the LSO and the MNTB being arranged from high to low in the medial-to-lateral direction. A very similar alignment of the tonotopic axes was subsequently found in the gerbil's LSO (Sanes et al. 1989) and in the rat's LSO and MNTB (Friauf 1992), and it is now generally assumed that the tonotopic organisation of the mammalian SOC nuclei is based on the same principle across species. The above-mentioned physiological results are in excellent agreement with a great number of anatomical findings, which have demonstrated topographical relations in the projections from and to the LSO (Irvine 1986; Cant 1991; Helfert et al. 1991), thus providing indirect evidence of tonotopicity in the LSO and the MNTB. Until now, however, there have been no data on the frequency organisation within the SPN, and therefore our data demonstrate a tonotopic organisation of this nucleus for the first time. The present results on the correlation between the BF of an MNTB principal cell and the location of its cell body, as well as its projection pattern into the LSO and the SPN, thus confirm and extend the previous literature, including most recent reports (Kuwabara and Zook 1991; Banks and Smith 1992).

Quantitative aspects of soma-dendritic and axonal morphology

The mean soma size of our injected MNTB neurons (14.3 μm × 21.9 μm) corresponded very well with the numbers determined by others in the rat (Harrison and Warr 1962, 15–18.5 μm; Banks and Smith 1992, 15.8 × 22.4 μm) and in other species (guinea pig, 10–15 μm × 25–30 μm, Schofield and Cant 1991; cat, 20 μm, Morest 1968); mouse, 17.5 μm, Ollo and Schwartz 1979), indicating that our intracellular recordings were not biased towards larger neurons. This conclusion is corroborated by the fact that the axonal diameter measured by us (1.6–1.7 μm) matches well with that reported by Harrison and Warr (1962) in the same species (1.1–2.25 μm). However, there is a discrepancy between our data and those of others (Spangler et al. 1985, 5–6 μm; Kuwabara and Zook 1991, 3–8 μm) which we cannot explain at present.

The observation that MNTB principal cells share many basic features across species is supported by the finding that each neuron from our sample of MNTB principal cells had one to two primary dendrites, confirming previous results in rodents and bats (Harrison and Warr 1962; Kuwabara and Zook 1991; Banks and Smith 1992) [Note, however, that two to four primary dendrites have been reported in cats (Morest 1968; Smith et al. 1989)]. Almost all of our neurons had dendritic fields that extended beyond the borders of the MNTB. This is in slight contrast to the results of Kuwabara and Zook (1991), who reported that two thirds of their labelled principal cells had intrinsic dendritic fields confined to the borders of the MNTB. Out of 29 of their remaining cells that had extrinsic dendritic fields, the dendrites of four crossed the midline and reached into the contralateral MNTB, something we never observed. Again, our sample size might be too small to identify this subpopulation of cells.

Physiological properties of MNTB principal cells

In contrast to the high number of anatomical studies on the MNTB, there have only been few physiological reports. The response patterns of MNTB cells to acoustic stimuli have been described most extensively by Guinan et al. (1972a,b). By far the most units recorded in the MNTB were monaurally excited by the contralateral ear (37 of 46) and responded in a tonic fashion (54 of 93), a pattern that we consistently observed as well. Whereas Guinan et al. (1972a) differentiated between two PSTH categories in the tonic response (see their categories A and B), we observed only one type of response and did not see a pronounced dip after the initial peak. The difference is likely to be due to the number of stimulus presentations used to compute the PSTHs (ten presentations at 1 Hz in the present study, 500 presentations at about 10 Hz in the study by Guinan et al.). Due to the low number of stimulus presentations, it remains unclear whether the recorded MNTB neurons presented the same response pattern as VCN globular bushy cells (i.e. primary-like with a notch).

There was a good correspondence between the response latencies reported in the cat (about 2.5–5.2 ms, Guinan et al. 1972a, see their Fig. 14, upper panel) and in the rat (3.3–3.9 ms, present study). Following intra-axonal recordings from the trapezoid body in rats, Friauf and Ostwald (1988) reported an average of 2.6 ms in globular bushy cells from the VCN, whose axons terminate on MNTB principal cells. If one adds 0.5 ms for synaptic

delay (Guinan and Li 1990), there is a reasonable match between the results.

The spontaneous activity recorded in the present study (109 spikes/s, range 95–123 spikes/s) was high and this was particularly striking, as MNTB principal cells do not appear to be spontaneously active in vitro (Banks and Smith 1992). The discrepancy initially suggested to us that the spontaneous activity might have been caused by injury following the penetration of the axons. However, extracellular in vivo studies have also indicated highly spontaneously active units in the MNTB (Guinan et al 1972a,b), and thus it is possible instead that non-spontaneously active MNTB neurons recorded in vitro are a result of the slicing procedure.

An unexpected result of our intracellular recordings was the shift of the membrane potential towards negative values when stimuli of high intensities were used. This result is particularly remarkable in view of the fact that all of our recordings were obtained from the proximal axons. There are three explanations for this phenomenon. First, the shift in the membrane potential could reflect an IPSP. GABAergic synapses have been identified on the somata of MNTB principal cells (Roberts and Ribak 1987; Adams and Mugnaini 1990), and they could generate IPSPs which would electrotonically spread from the soma and be picked up by our recording electrodes. However, this assumption seems rather unlikely, because we never observed EPSPs – which are likely to be of huge amplitude due to the axosomatic synapse formed by each calyx of Held. We therefore conclude that electrotonically diminished subthreshold postsynaptic potentials originating in the soma were too weak to be picked up by our electrodes. Second, biophysical properties of the axon membrane could result in activity-dependent conductance changes (such as opening of Cl^- or K^+ channels), resulting in more negative membrane potentials. Hyperpolarising voltage shifts during stimulation were not seen in vitro, even if the neurons generated action potentials at a similarly high frequency as did our cells (Banks and Smith 1992). However, as the in vitro recordings were obtained from the somata, one cannot at present exclude the possibility that biophysical membrane properties of the axon play a part. Nevertheless, we think that the third possibility is most plausible: inhibitory synapses terminating directly at the proximal axon of an MNTB principal cell could generate powerful IPSPs, which could be strong enough to be picked up by our recording electrodes, even after being electrotonically augmented. Unfortunately, in spite of several EM studies in rats (Lenn and Reese 1966; Casey and Feldman 1985, 1988), there are no data on synaptic contacts on axons of MNTB principal cells which would confirm this theory. Therefore, the underlying mechanism for the hyperpolarisation during the stimulus remains open.

Conclusion

Single MNTB principal cells have a complex system of axonal projections reaching a variety of brainstem nuclei that process information in the ascending and – to a minor degree – in the descending auditory system. Because of these complex, divergent projections it is highly likely that these cells play a more complex role than simply being a sign-converting relay station between the contralateral ventral cochlear nucleus and the lateral superior olive, as originally suggested by Spangler et al. (1985). A hypothetical microcircuit in the rat auditory brainstem, in which MNTB principal neurons play a pivotal role, is shown in Fig. 13. From this microcircuit, it is obvious that most of the contralateral SOC nuclei are in a position to receive short-latency acoustic input from the *contralateral* ear, either monosynaptically from globular bushy neurons or disynaptically via MNTB principal cells. Together with the excitatory, monosynaptic input that SOC neurons receive from the *ipsilateral* ear (via the VCN, not completely shown), this results in a complex scenario of, as yet unknown, synaptic interactions.

A further possible role for MNTB principal cells that can be deduced from Fig. 13 is the possibility that they may be involved in "feedforward inhibition". They receive excitatory input from globular bushy cells in the contralateral VCN and inhibit VNLL neurons, which in turn may be excited by globular bushy cells. This assumption, however, is still speculative as the type of VNLL neurons that are postsynaptic to globular bushy cells in the contralateral VCN and to MNTB principal cells is still unknown. Further morphological studies at the single-cell level and at the ultrastructural level, and/or electrophysiological studies are required to untangle the puzzling micro-anatomy of the auditory brainstem nuclei. As MNTB principal cells have been recognised in all mammalian species examined (see Kuwabara and Zook 1991) and as all the above-mentioned physiological and morphological data are in favour of a very similar organisation of these neurons across the mammalian group, studies in all species should be able to contribute valuable results in this adventure.

Acknowledgements. This work was supported by a grant from the Deutsche Forschungsgemeinschaft to E.F. (Fr 772/1-2) and by a scholarship from the Graduiertenkolleg Neurobiologie Tübingen to K.L. Experimental work reported in this article fulfilled partial requirements for completion of a masters thesis (I.S.) in the Department of Animal Physiology, University of Tübingen. Thanks to Martina Hohloch for photographic assistance, and special thanks to Gwynn Goldring for correcting our English.

References

Adams JC (1981) Heavy metal intensification of DAB-based reaction product. J Histochem Cytochem 29:775

Adams JC, Mugnaini E (1990) Immunocytochemical evidence for inhibitory and disinhibitory circuits in the superior olive. Hearing Res 49:281–298

Aschoff A, Ostwald J (1987) Different origins of cochlear efferents in some bat species, rats, and guinea pigs. J Comp Neurol 264:56–72

Banks MI, Smith PH (1992) Intracellular recordings from neurobiotin-labelled cells in brain slices of the rat medial nucleus of the trapezoid body. J Neurosci 12:2819–2837

Bledsoe SC Jr, Pandya P, Altschuler RA, Helfert RH (1988) Axonal projections of PHA-L-labeled neurons in the medial nucleus of the trapezoid body. Soc Neurosci Abstr 14:491

Borg E (1973) A neuroanatomical study of the brainstem auditory system of the rabbit. I. Ascending connections. Acta Morphol Neerl-Scand 2:31–48

Browner RH, Webster DB (1975) Projections of the trapezoid body and the superior olivary complex of the kangaroo rat (*Dipodamys merriami*). Brain Behav Evol 11:322–354

Caird D, Klinke R (1983) Processing of binaural stimuli by cat superior olivary complex neurons. Exp Brain Res 52:385–399

Cant NB (1991) Projections to the lateral and medial superior olivary nuclei from the spherical and globular bushy cells of the anteroventral cochlear nucleus. In: Altschuler RA, Bobbin RP, Clopton BM, Hoffman DW (eds) Neurobiology of hearing: the central auditory system. Raven Press, New York, pp 99–119

Casey MA, Feldman ML (1982) Aging in the rat medial nucleus of the trapezoid body. I. Light microscopy. Neurobiol Aging 3:187–195

Casey MA, Feldman ML (1985) Aging in the rat medial nucleus of the trapezoid body. II. Electron microscopy. J Comp Neurol 232:401–413

Casey MA, Feldman ML (1988) Age-related loss of synaptic terminals in the rat medial nucleus of the trapezoid body. Neuroscience 24:189–194

Caspary DM, Finlayson PG (1991) Superior olivary complex: functional neuropharmacology of the principal cell types. In: Altschuler RA, Bobbin RP, Clopton BM, Hoffman DW (eds) Neurobiology of hearing: the central auditory system. Raven Press, New York, pp 141–161

Elverland HH (1978) Ascending and intrinsic projections of the superior olivary complex in the cat. Exp Brain Res 32:117–134

Friauf E (1986) Morphology of motoneurons in different subdivisions of rat facial nucleus stained intracellularly with horseradish peroxidase. J Comp Neurol 253:231–241

Friauf E (1992) Tonotopic order in the adult and developing auditory system of the rat as shown by c-fos immunocytochemistry. Eur J Neurosci 4:798–812

Friauf E, Ostwald J (1988) Divergent projections of physiologically characterized rat ventral cochlear nucleus neurons as shown by intraaxonal injection of horseradish peroxidase. Exp Brain Res 73:263–284

Glendenning KK, Brunso-Bechtold JK, Thompson GC, Masterton RB (1981) Ascending auditory afferents to the nuclei of the lateral lemniscus. J Comp Neurol 673:703

Glendenning KK, Hutson KA, Nudo RJ, Masterton RB (1985) Acoustic chiasm II: anatomical basis of binaurality in the lateral superior olive of the cat. J Comp Neurol 232:261–285

Guinan JJ Jr, Li RY-S (1990) Signal processing in brainstem auditory neurons which receive giant endings (calyces of Held) in the medial nucleus of the trapezoid body of the cat. Hearing Res 49:321–334

Guinan JJ Jr, Guinan SS, Norris BE (1972a) Single auditory units of the superior olivary complex. I. Responses to sounds and classifications based on physiological properties. Int J Neurosci 4:101–120

Guinan JJ Jr, Norris BE, Guinan SS (1972b) Single auditory units in the superior olivary complex. II. Locations of unit categories and tonotopic organization. Int J Neurosci 4:147–166

Harrison JM, Warr WB (1962) A study of the cochlear nuclei and ascending auditory pathways of the medulla. J Comp Neurol 119:341–380

Held H (1893) Die zentrale Gehörleitung. Arch Anat Physiol 17:201–248

Helfert RH, Snead CR, Altschuler RA (1991) The ascending auditory pathways. In: Altschuler RA, Bobbin RP, Clopton BM, Hoffman DW (eds) Neurobiology of hearing: the central auditory system. Raven Press, New York, pp 1–25

Irvine DRF (1986) Progress in sensory physiology 7. The auditory brainstem. Springer, Berlin Heidelberg New York

Itoh K, Konishi A, Nomura S, Mizuno N, Nakamura Y, Sugimoto T (1979) Application of coupled oxidation reaction to electron microscopic demonstration of horseradish peroxidase: cobalt-glucose method. Brain Res 175:341–346

Kelly JB, Masterton RB (1977) Auditory sensitivity of the albino rat. J Comp Physiol Psychol 91:930–936

Kuwabara N, Zook JM (1991) Classification of the principal cells of the medial nucleus of the trapezoid body. J Comp Neurol 314:707–720

Kuwabara N, DiCaprio RA, Zook JM (1991) Afferents to the medial nucleus of the trapezoid body and their collateral projections. J Comp Neurol 314:684–706

Lenn NJ, Reese TS (1966) The fine structure of nerve endings in the nucleus of the trapezoid body and the ventral cochlear nucleus. Am J Anat 118:375–390

Lingenhöhl K, Friauf E (1991) Sensory neurons and motoneurons of the jaw-closing reflex pathway in rats: a combined morphological and physiological study using the intracellular horseradish peroxidase technique. Exp Brain Res 83:385–396

Lingenhöhl K, Friauf E (1992) Giant neurons in the caudal pontine reticular formation receive short latency acoustic input: an intracellular recording and HRP study in the rat. J Comp Neurol 325:473–492

Moore MM, Caspary DM (1983) Strychnine blocks binaural inhibition in lateral superior olivary neurons. J Neurosci 3:237–242

Morest DK (1968) The collateral system of the medial nucleus of the trapezoid body of the cat, its neuronal architecture and relation to the olivo-cochlear bundle. Brain Res 9:288–311

Ollo C, Schwartz IR (1979) The superior olivary complex in C57BL/6 mice. Am J Anat 155:349–374

Roberts RC, Ribak CE (1987) GABAergic neurons and axon terminals in the brainstem auditory nuclei of the gerbil. J Comp Neurol 258:267–280

Saint Marie RL, Ostapoff E-M, Morest DK, Wenthold RJ (1989) Glycine-immunoreactive projection of the cat lateral superior olive: possible role in midbrain ear dominance. J Comp Neurol 279:382–396

Sanes DH, Siverls V (1991) Development and specificity of inhibitory terminal arborizations in the central nervous system. J Neurobiol 8:837–854

Sanes DH, Merickel M, Rubel EW (1989) Evidence for an alteration of the tonotopic map in the gerbil cochlea during development. J Comp Neurol 279:436–444

Schofield BR, Cant NB (1991) Organization of the superior olivary complex in the guinea pig. I. Cytoarchitecture, cytochrome oxidase histochemistry, and dendritic morphology. J Comp Neurol 314:645–670

Schofield BR, Cant NB (1992) Projections to the cochlear nucleus from principal cells in the medial nucleus of the trapezoid body. Soc Neurosci Abstr 18:1039

Smith PH, Joris PX, Banks MI, Yin TCT (1989) Physiology and anatomy of principal cells in the cat MNTB. Soc Neurosci Abstr 15:746

Smith PH, Joris PX, Carney LH, Yin TCT (1991) Projections of physiologically characterized globular bushy cell axons from the cochlear nucleus of the cat. J Comp Neurol 304:387–407

Sommer I, Lingenhöhl K, Friauf E (1992) Characterization of principal neurons in the rat medial nucleus of the trapezoid body by intracellular recording and labeling. Soc Neurosci Abstr 18:1037

Spangler KM, Warr WB, Henkel CK (1985) The projections of principal cells of the medial nucleus of the trapezoid body in the cat. J Comp Neurol 238:249–262

Spirou GA, Brownell WE, Zidanic M (1990) Recordings from cat trapezoid body and HRP labeling of globular bushy cell axons. J Neurophysiol 63:1160–1190

Taber E (1961) The cytoarchitecture of the brainstem of the cat. J Comp Neurol 116:27–69

Tsuchitani C, Boudreau JC (1966) Single unit analysis of cat superior olive S segment with tonal stimuli. J Neurophysiol 29:684–697

Warr WB (1972) Fiber degeneration following lesions in the multi-

polar and globular cell areas in the ventral cochlear nucleus of the cat. Brain Res 40:247–270

Wenthold RJ (1991) Neurotransmitters of brainstem auditory nuclei. In: Altschuler RA, Bobbin RP, Clopton BM, Hoffman DW (eds) Neurobiology of hearing: the central auditory system. Raven Press, New York, pp 121–139

White JS, Warr WB (1983) The dual origins of the olivocochlear bundle in the albino rat. J Comp Neurol 219:203–214

Winter IM, Robertson D, Cole S (1989) Descending projections from auditory brainstem nuclei to the cochlea and cochlear nucleus of the guinea pig. J Comp Neurol 280:143–157

Wu SH, Kelly JB (1992) NMDA, non-NMDA and glycine receptors mediate binaural interaction in the lateral superior olive: physiological evidence from mouse brain slice. Neurosci Lett 134:257–260

Zook JM, DiCaprio RA (1988) Intracellular labeling of afferents to the lateral superior olive in the bat, *Eptesicus fuscus*. Hearing Res 34:141–148